

Light Localization Effect on the Optical Properties of Opals Doped with Gold Nanoparticles

Valentina Morandi,[†] Franco Marabelli,[†] Vincenzo Amendola,[‡] Moreno Meneghetti,[‡] and Davide Comoretto^{*,§}

Dipartimento di Fisica "A.Volta", Università degli Studi di Pavia, via Bassi 6, 27100 Pavia, Italy, Dipartimento di Scienze Chimiche, Università degli Studi di Padova, via Marzolo 1, 35131 Padova, Italy, and Dipartimento di Chimica e Chimica Industriale, Università degli Studi di Genova, via Dodecaneso 31, 16146 Genova, Italy

Received: November 20, 2007; In Final Form: February 19, 2008

Polystyrene artificial opals having both different microsphere diameters and gold nanoparticles (AuNP) doping levels have been prepared and their spectroscopic characterization has been performed. Reflectance spectra of doped opals show a red shift of the photonic band gap and a reduction of its width and intensity upon increasing AuNP doping level, but they do not show any direct evidence of AuNP plasmon resonance. Transmittance spectra of the same samples recorded on the same spot area show, instead, a doping level dependent line shape. For the highest doping level a complicated sigmoidal line shape due to the overlap of broad AuNP absorption and photonic crystal stop band is observed. This unusual effect is accounted for by considering the localization of standing electromagnetic waves within both the microspheres and the interstices where the AuNP are embedded.

Introduction

Among photonic crystals (PC), i.e., materials possessing a periodical modulation of the dielectric constant on a scale length comparable to the wavelength of visible light, artificial opals are a simple, cheap, and interesting playground to investigate optical effects on this class of materials. Despite opals not showing a complete photonic band gap (PBG) but only a pseudogap (stop band), their versatility allows interesting structures to be obtained. As a matter of fact, they can be employed as templates to prepare inverse opals (which instead might have a complete PBG) and they can be easily infiltrated with a variety of materials ranging from metals to organic semiconductors.¹

Concerning the infiltration with metallic systems, we can roughly distinguish between two approaches. One is the infiltration with bulk metals^{2–5} while the other is the infiltration with metallic nanoparticles.^{6–14} The first approach exploits the Drude-like behavior of the metal dielectric constant close to the plasma frequency to obtain an inverse opal having a large dielectric contrast, which favors the opening of a complete photonic band gap. Moreover, such composite photonic crystals might become, in a suitable spectral range, a transparent system possessing a high electric conductivity. Tailoring of the photonic band structure provided by metal (i.e., redistribution of electromagnetic field density of states into the photonic crystal) can also substantially modify the blackbody spectrum emitted thus enhancing thermal emission in the visible spectrum and allowing the engineering of novel and efficient light sources. Metallic nanoparticles as a medium for infiltration or for preparation of inverse opals has attracted much attention due to their importance in the field of catalysis, sensing, and photonics.^{6,7,9,11–15}

In this respect, several papers have been devoted to opals used as a template for infiltration of metallic composite nanoparticles. Only in a few papers^{6,7} have the optical properties of such systems been investigated focusing on the role of surface plasmon resonance and/or photonic band gaps when well separated in energy. Our interest is the spectroscopy of opals doped in a controlled manner with gold nanoparticles (AuNP), which instead show some overlap between the surface plasmon resonance of the AuNP and the photonic stop band. In a previous work, we have reported that weakly AuNP-doped opals show an interesting optical switching effect when resonantly photo-excited with a modification of transmittance at the stop band of about 150% in the nanosecond time regime.⁸ In this paper we focus our attention on AuNP highly doped opals whose transmittance spectra show, for the signature associated with the stop band, an unusual line shape due to a particular effect of light localization. Different mechanisms for light localization have been reported so far. For instance, localization due to disorder^{16,17} or engineered defect¹⁸ of the three-dimensional (3D) opal structure is known to confine the electromagnetic field inside the photonic crystal. Here, we find a case of light localization that can be useful in preparing new materials for photonics: the formation of stationary waves for photon energies close to both the high (air band) and low energy (dielectric band) border of the stop band. In this case the electromagnetic field of impinging light is standing, i.e., localized, in the opal microspheres or in its interstices without propagation.¹⁹ In our system, when the photonic stop band is tuned on the broad surface plasmon resonance of AuNP a novel fingerprint is observed in transmittance spectra thus providing a simple tool to evaluate the achievement of the localization conditions. Notice that when such a condition is obtained, the group velocity of light is reduced and then the interaction time of photons with the photonic crystal is increased. In the case of opals, when the interstices are infiltrated with photoactive materials, such as molecules suitable for lasing or nonlinear optics, the extended

* To whom correspondence should be addressed. E-mail: comoretto@chimica.unige.it.

[†] Università degli Studi di Pavia.

[‡] Università degli Studi di Padova.

[§] Università degli Studi di Genova.

time of interaction between active material and localized (standing) light provides a new tool for lowering all threshold processes with respect to bulk materials, i.e., for tailoring the properties of the materials.

Results and Discussion

AuNP were prepared by laser ablation^{20–23} in water solutions of sodium dodecyl sulfate (10^{12} AuNP/cm³). Their average diameter was determined by fitting the UV–vis solution spectra with the Mie–Gans model, which was shown to be a simple and reliable method.^{20–23} It was found that AuNP have an average diameter of 10 nm, which is small enough to be included in the interstices of opals without perturbing their structure. Polystyrene (PS) opals, both bare and AuNP doped, were grown according to the procedure previously reported.⁸ The AuNP doping level of opals is determined by the AuNP amount inside the polystyrene microsphere suspensions (Duke Scientific) used for opal growth. We prepared opals with two PS microsphere diameters ($a = 260$ and 300 nm) and with three different AuNP concentrations, determined in order to have, in the growth suspensions, about 2 AuNP for 100, 10, and 1 microspheres. Samples grown with such suspensions are labeled as low loading (LL), medium loading (ML), and high loading (HL) opals, respectively. We observed that the deposition kinetics of AuNP is faster than that of microspheres so that, in the early stage of sample formation, the infiltration degree is higher than that calculated, whereas an almost bare opal grows at the end. As a consequence we also found that in the infiltrated part of the opal (several millimeters long), the AuNP concentration is not perfectly uniform, being slowly increasing along the growth direction. Then the infiltration process suddenly stops and a bare opal is grown.⁸ However, on the scale length of the probing spot (100 μm diameter) the opal is very uniform and nice interference fringes are observed in optical spectra thus indicating the good optical quality of the sample (see below).

Figure 1 compares the reflectance (R) spectra of bare opals with those for opals having different AuNP doping levels, both for 260 and 300 nm spheres. Bare opals of 260 nm spheres (Figure 1a) show the typical reflectance peak (Bragg peak) due to backward diffraction of incident light by the photonic crystal at 17305 cm^{-1} (578 nm) as well as well-pronounced interference fringe patterns due to reflection from the backside of the sample. The spectral position of the Bragg peak (the fingerprint of all photonic crystals) bathochromically shifts upon increasing the AuNP doping, as expected for infiltration with a dielectric medium. In particular for LL, ML, and HL 260 nm opals the peak is observed at 16601 (602 nm), 15843 (631 nm), and 15571 cm^{-1} (642 nm), respectively. Furthermore, all spectra show interference fringes (both below and above the energy of the Bragg peak) for any AuNP doping level, thus indicating the good optical quality also for doped opals. We also notice that, upon increasing the AuNP doping level, the intensity of the reflectance peak decreases and its full-width half-maximum (fwhm) is reduced. These effects already have been discussed and accounted for.⁸ Similar results are observed for 300 nm opals (Figure 1b) where the Bragg peaks are spectrally shifted according to the scaling laws of photonic crystals.¹⁹ Indeed the Bragg peak for bare, LL, ML, and HL doping samples is observed at 14813 (675 nm), 13928 (718 nm), 13783 (725 nm), and 13320 cm^{-1} (751 nm), respectively. Notice that from all these spectra no evidence of spectral features due to AuNP plasmon resonance is detected.

We notice that such spectra can be unambiguously interpreted in terms of infiltration with a dielectric material possessing a

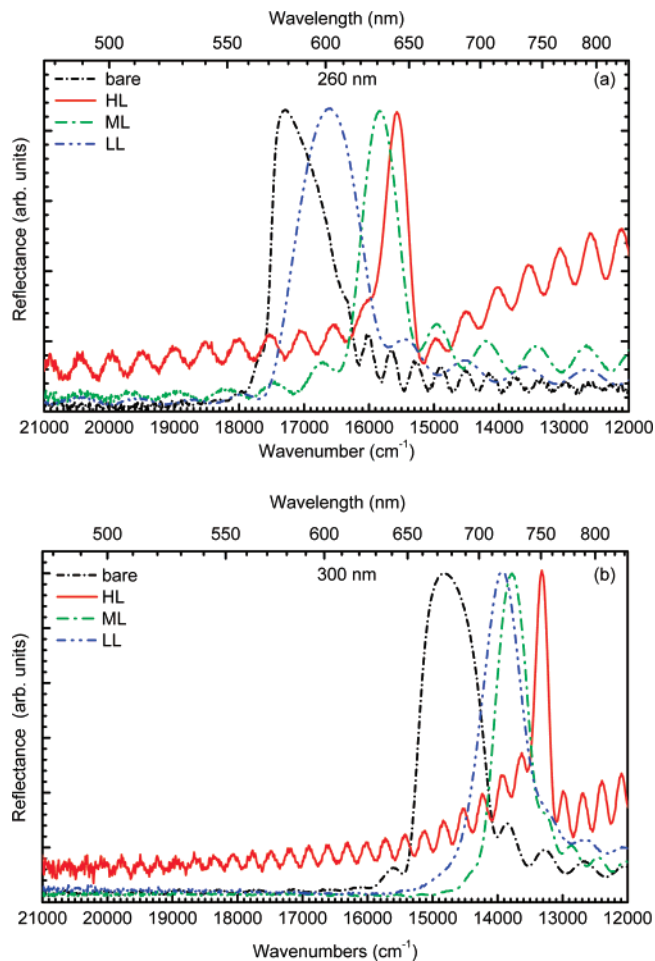


Figure 1. Near-normal incidence (5°) reflectance spectra (TM polarization) for 260 (a) and 300 nm (b) bare and different AuNP doped opals. All spectra are normalized at the peak intensity.

real dielectric constant. Indeed, reflectance spectra do not comply with those predicted for metallic photonic crystals where the dielectric constant has a negative real part and a small imaginary one, which induces a strong reduction of photonic band dispersion with the appearance of a cutoff frequency and a dramatic decrease of the reflectance intensity for photon energies higher than that of the cutoff.^{24,25}

Figure 2 reports, for the same samples, the transmittance (T) spectra recorded in the same spot area used for R measurements.²⁶ For 260 nm bare opals the T minimum is detected at 17105 cm^{-1} (585 nm) while for LL opals it is at 16717 cm^{-1} (598 nm), in agreement with above findings observed in R spectra. For ML opals the shape of the T spectrum is modified into a broad background band ($15000\text{--}21000\text{ cm}^{-1}$) with a weak dip at about 15872 cm^{-1} (630 nm). This weak dip occurs almost at the same wavelength of the peak of the R spectrum for the same sample (Figure 1a). If the AuNP doping level is further increased (HL samples), the background becomes more pronounced and broader ($21000\text{--}12000\text{ cm}^{-1}$) and the weak dip becomes a sigmoidal structure whose center (indicated by an arrow in Figure 2a) is located at 15580 cm^{-1} (642 nm). The broad T background is very similar to the absorption spectrum of aggregated AuNP as observed both in solutions^{20,21} and in AuNP doped opals after solubilization of the PS microspheres.⁸ This fact further supports our previous findings that the infiltration occurred with nanoparticles and not with bulk metal. We point out that this effect is not observed in the R spectra thus suggesting that its origin is due to an absorption process by AuNP. More puzzling is the origin of the sigmoidal structure,

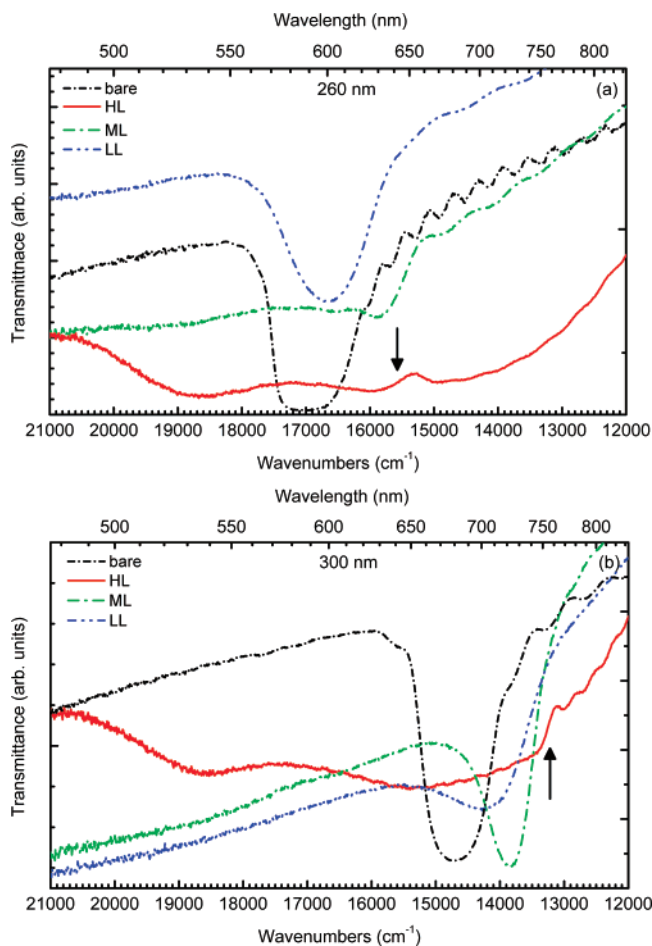


Figure 2. Normal incidence transmittance spectra for 260 (up) and 300 nm (down) bare and different AuNP doped opals.

which is the main interest of this work. We notice that the center of this feature matches the Bragg peak of the corresponding R spectrum, thus suggesting some correlation with the photonic pseudogap (see below).

T spectra recorded for 300 nm samples (Figure 2b) have similar behavior to those described for 260 nm opals except for the bathochromic shift associated with the scaling laws of PCs. For bare, LL, and ML opals the minima are detected at 14721 (679 nm), 14229 (703 nm), and 13870 cm^{-1} (721 nm), respectively, and favorably compare with the spectral position of the Bragg peak in the R spectra for corresponding samples.

For 300 nm HL opals, a double minima (18644–536 nm, 15317–653 nm) broad background absorption is again observed and the sigmoidal structure is overlapped to the steep part of the T spectrum at about 13222 cm^{-1} (756 nm), thus giving it a pronounced step-like character. One again notice that the center of the sigmoidal structure is located at the same wavelength of the Bragg peak in the R spectra.

The energy shift of the stop band observed in the R and T spectra can be related to the concentration of AuNP inside the opal interstices. In fact, the infiltration of AuNP modifies the PC dielectric contrast, increasing the refractive index of interstices and then the effective refractive index (n_{eff}) of the photonic crystal. The spectral position of the observed sigmoidal structure also appears to follow such a dependence, with respect to either the doping level or the PS sphere diameter.

Very intriguing is the presence and nature of the sigmoidal structure. The correspondence observed between the center of the sigmoidal feature and the Bragg peak in R spectra, as well as the scaling properties of its spectral position with the sphere

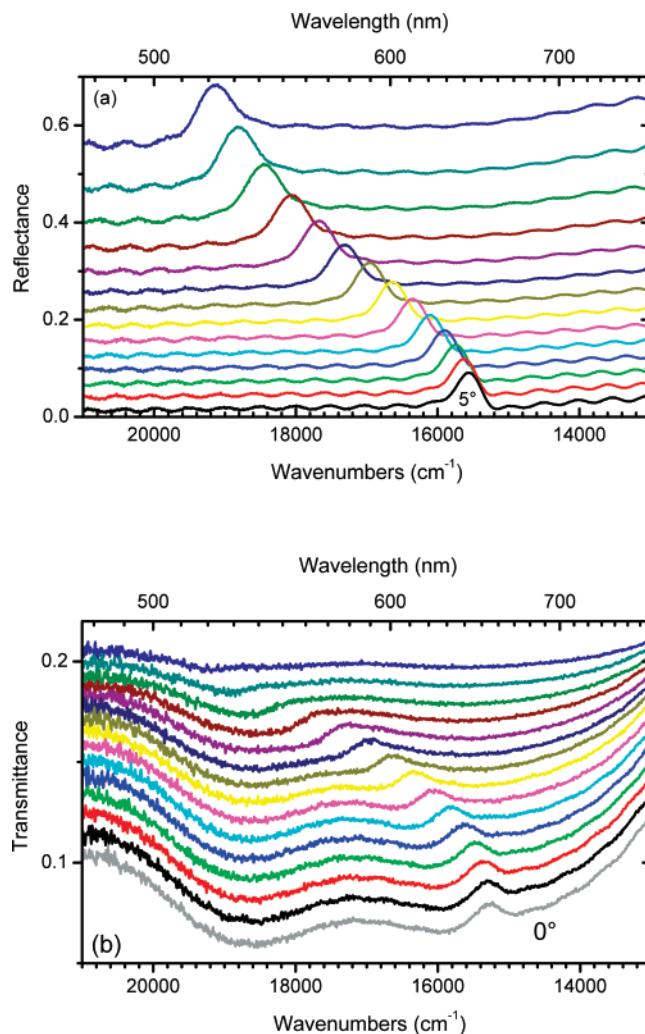


Figure 3. Dispersion properties of 260 nm HL AuNP doped opals both for reflectance (a) and transmission (b) for TE polarization. Spectra, recorded every 5°, are offset for clarity.

diameter, strongly suggests the correlation with the photonic stop band. To demonstrate this assignment, we recorded on the same spot area R and T spectra at different incidence angles for TE polarization²⁷ and for all samples. Such spectra are reported and compared in Figure 3 for 260 HL opals where the effect of sigmoidal structure is more pronounced and evident.

Figure 3a shows the dispersion of the photonic stop band with a progressive ipsochromic shift of the peak upon increasing the incidence angle. In the transmittance spectra (Figure 3b) the sigmoidal structure also shifts toward higher energies upon increasing the incidence angle in full agreement with the dispersion of the stop band observed in reflectance spectra (Figure 3a). The position of the stop band ($\lambda_{\text{stop band}}$) can be simply related to the incidence angle (θ) through the effective refractive index (n_{eff}) of the opals and to the interplanar spacing (D) by the well-known Bragg–Snell law ($\lambda_{\text{stop band}} = 2D(n_{\text{eff}}^2 - \sin^2 \theta)^{0.5}$, where $D = a(2/3)^{0.5}$ is fixed by the sphere diameter).²⁸ This formula is used to obtain n_{eff} by fitting the dispersion of the peak observed in the R spectra (Figure 3a) and the dispersion of the sigmoidal feature observed in the T spectra (Figure 3b) averaged over TE and TM polarizations. In both cases, we found the same effective refractive index within the experimental error (see Figure 4), in particular, for 260 (300 nm) n_{eff} is 1.42 (1.43), 1.49 (1.49), and 1.52 (1.53) for LL, ML, and HL opals, respectively. In the framework of the Lorentz–Lorenz theory for the effective medium,^{8,29} these values for n_{eff}

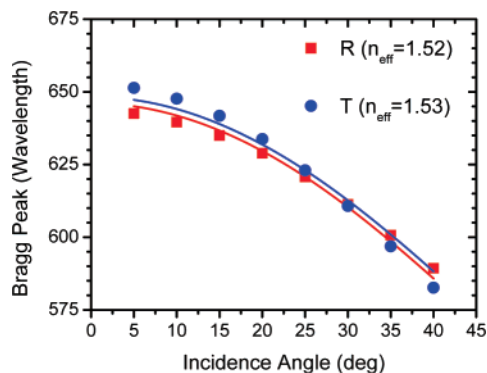


Figure 4. Dispersion of reflectance peak (red squares) and sigmoidal structure (blue circles) as a function of the incidence angle. Lines are fitted with the Bragg–Snell law. Data are averaged over TE and TM polarizations.

correspond to a change of the dielectric constant of interstices between spheres with respect to the case of bare opals of 3% (9%), 50% (50%), and 77% (86%) for LL, ML, and HL opals, respectively. Since the results obtained for the center of the sigmoidal feature are very similar of those for the peak in the R spectra, we unambiguously assign the sigmoidal feature to the photonic band structure even though it possesses an unusual shape.

Besides this structure, which disappears at the highest incidence angles, a background absorption, almost independent of polarization and incidence angle, can be observed with two minima located at 18885 (530 nm) and 15800 cm^{-1} (633 nm). From the comparison of the transmittance spectra of infiltrated opals with those of AuNP solutions,⁸ we assign the double minima in transmission to the absorption of spherical (about 18800 cm^{-1}) and spheroidal (at 15800 cm^{-1}) AuNP. According to this interpretation and comparing the intensities of the two bands, we deduce that the amount of spheroidal AuNP inside the interstices of the opals is much increased with respect to that existing in the suspension used to grow opals. This fact is reasonable since, during opal growth, evaporation of water allows a greater AuNP interaction, thus giving rise to aggregates whose typical absorption is close to the low-energy side of the visible spectral region.

The explanation for the unusual line shape of the sigmoidal feature observed in T spectra is possible taking into account the effect of AuNP absorption joined to the localization of the electromagnetic field close to the band gap. In Figure 5 we compared T spectra with the photonic band (PBG) structure calculated for our opals.³⁰ At the pseudogap in the L point of the Brillouin zone, the photonic bands are almost flat (see Figure 5c), thus making the effective refractive index divergent and then slowing down to zero the group velocity of the light, i.e., generating a stationary wave. In these conditions, the electromagnetic field in the air band, namely the high-energy photonic band, is mainly localized in the low dielectric constant material (Figure 5a), whereas the electromagnetic field of the dielectric band, the low-energy photonic band, is mainly localized in the high dielectric constant material.¹⁹ In the present case, the high dielectric constant material is represented by the PS spheres ($\epsilon = 2.53$) and the low dielectric constant material by the interstices infiltrated with the AuNP particles since we have found above that their dielectric constant is in the range 1.03–1.86. Therefore, one can predict that a lower absorption is operating in the dielectric band since the electromagnetic field is localized where the transparent PS spheres are present. On the contrary, a larger absorption can be found for the air band since in this case the electromagnetic field is localized where the absorbing

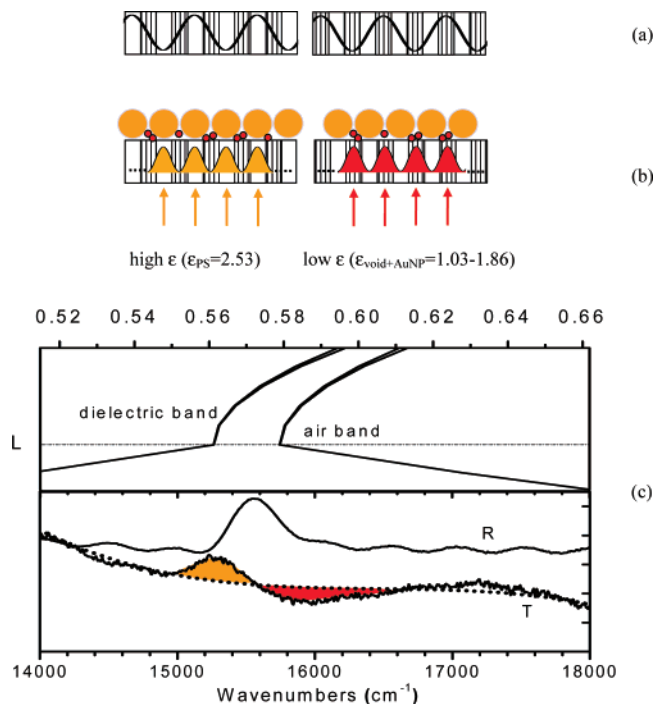


Figure 5. Sketch of electric field localization in the high (low) dielectric constant materials for a one-dimensional photonic crystal when photon frequency approaches dielectric (air) bands (left and right, respectively) at the photonic gap (a) and same sketch for the energy of the electromagnetic field (b). Big yellow balls represent PS microspheres ($\epsilon_{\text{PS}} = 2.53$) while red dots correspond to AuNP ($\epsilon_{\text{void+AuNP}} = 1.03\text{--}1.86$ depending on the doping level). Comparison of the calculated photonic band structure of a HL infiltrated opal with experimental R and T spectra (c). The yellow (red) dashed area indicates reduction (increase) of absorption due to PS microspheres (AuNP).

AuNP are present. This explains (see Figure 5c) the structure of the sigmoidal feature that reflects a higher absorption (red area), with respect to the background, at higher frequency and a lower absorption (yellow area) at lower frequency.

A possible objection to our reasoning could be due to the limited thickness of the samples, which could reduce the interaction of photons with the photonic crystal and then with the active material there embedded. We then compared the Bragg attenuation length L_B , i.e., the attenuation per unit length of transmitted wave in a photonic crystal for frequencies within the stop band, with the sample thickness obtained from the interference fringes. Usually L_B is obtained by coherent back-scattering measurements³¹ or by measuring the transmitted light intensity attenuation in samples having different thickness.^{32,33} This last method is unuseful in our case, due to the change of the line shape in transmission spectra observed upon increasing the AuNP doping level. In principle, L_B can also be deduced from the relative width of the stop band in reflectance measurements

$$L_B = \frac{2DE_B}{\pi\Delta E} \quad (1)$$

where D is the interplanar spacing previously defined, E_B the stop band energy, and ΔE its full-width half-maximum. This method might be affected by defects which broaden the stop band^{31,34} thus making the values of L_B obtained from eq 1 quite rough. However, we adopted this approach being aware of its limits but also of the better optical quality of our samples (due to reduced thickness, 7 μm , and pronounced interference fringes) with respect to those used in literature (about 100 μm thick).

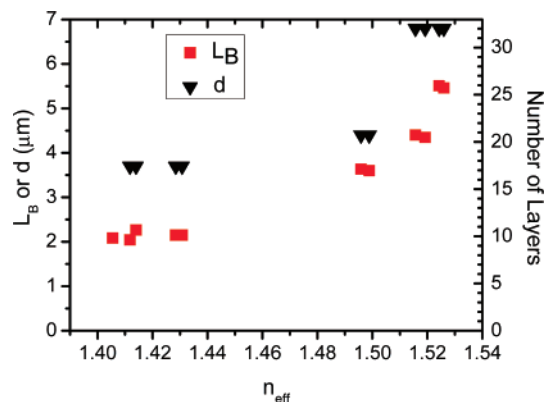


Figure 6. Comparison of Bragg attenuation length (L_B) and thickness (d ; left scale, μm ; right scale, number of sphere layers) for different AuNP doped opals.

As a matter of fact, the quality test for our bare opals is the reduced broadening, $\Delta E/E_B < 0.05$, with respect to the value 0.09 reported in previous papers. Notice also that for infiltrated opals $\Delta E/E_B$ is even further decreased.

We then determined L_B for all our 260 nm opals at different AuNP doping levels and we compared those values with the sample thickness determined from the interference fringes (see Figure 6). Notice that all these data have been measured on the same spot area (100 μm diameter).

The values of L_B obtained favorably compare with those reported in the literature for PS opals infiltrated with Rhodamine³⁵ (1.5–2 μm) or Coumarine dyes³³ (2 μm) and for silica opals³⁶ (5.1 μm). We also notice that in all cases, $L_B < d$, thus indicating that light propagating inside the stop band is attenuated by coherent Bragg scattering independently of the AuNP doping level and thus confirming that photons are allowed to interact with the photonic crystal and then with AuNP in agreement with our interpretation. In addition, by considering that photons are back reflected from interfaces, as testified by the interference fringes, further room for photon–opal interaction is provided. A further confirmation that our opal films are thick enough to demonstrate fully developed photonic crystal properties can be obtained in the literature^{37,38} where it is demonstrated that opals 20 sphere layers thick already possess photonic properties fully developed and very close to that of bulk samples. Notice that our HL opals are more than 25 layers thick, then we expect that photons traveling within such samples with energy in the stop band are coherently diffracted by the photonic crystal and that all optical effects observed are intrinsic to the photonic band structure and not due to artifacts.

Finally, we would like to notice that for HL samples, the reflectivity data show that $\Delta E/E_B = 0.02$ – 0.03 in full agreement with the values calculated from the band structure reported in Figure 5 (0.035) thus confirming in an independent way that the approximation used for our band structure calculations are reasonable.

A general comment on unusual line shapes observed in optical spectra of infiltrated opals could also be useful. A complicated reflectivity line shape has been reported in dye infiltrated opals and attributed to braggoritons,³⁹ i.e., excitations due to the interaction of excitons and coherent Bragg diffracted photons. Even though we cannot definitively exclude the role of such light matter interaction mechanisms for our samples, we notice that Braggoritons have been unambiguously observed when a very sharp excitonic absorption is tuned over a broader photonic stop band for a thick opal^{39,40} and no sigmoidal feature has been predicted in that case.⁴¹ In AuNP doped opals, all spectral

features due to surface plasmon are instead very broad. Moreover, braggoritons or similar excitations like polaritons^{42–44} show a branching of optical modes between excitonic and photonic bands possessing different dispersion and polarization properties. Our data instead show a single dispersive unpolarized spectral feature with different line shapes for reflectance or transmittance spectra. For these reasons we feel that our interpretation, related to standing waves inside the sample, is to be preferred.

To the best of our knowledge, this is the first report of the effect of light localization in the transmittance spectra of the photonic crystal of opals infiltrated with low absorbing materials. This result is particularly stimulating since this effect can be further exploited with infiltrating materials possessing large nonlinear optical or lasing properties. In this case, light localization in the spatial region where active material is infiltrated might allow optical thresholds to be reduced to activate harmonic generation, optical limiting, switching effects, or lasing, as already observed in one-dimensional photonic structures,^{45–49} since the interaction time of photons with the crystal is enhanced. A possible strategy to obtain such three-dimensional nanophotonics systems can be the functionalization of microspheres and/or gold nanoparticles with nonlinear active molecules.

Conclusions

We found experimental evidence of the effect of light localization on the optical properties of PS artificial opals doped with gold nanoparticles. For low AuNP concentrations the effect of doping is the same as that of infiltration with a dielectric material, i.e., a bathochromic shift of the Bragg peak, joined to a reduction of its fwhm and a lowering of its intensity. For the HL doping level, however, the AuNP plasmon absorption cannot be neglected and a remarkable difference between R and T spectra is observed. A sigmoidal structure, whose spectral position and dispersion properties are similar to those observed in R for the Bragg peak, is overlapped to the broad background due to the absorption of the plasmon band of AuNP. The line shape of this structure has been recognized to be the signature of light localization inside the PC. In the air band, when the electromagnetic field is localized within the interstices among microspheres, the absorption increases due to the presence of absorbing AuNP. When instead the electromagnetic field is localized within the PS microspheres (dielectric band), the absorption is reduced since PS is transparent. This effect, due to the photonic crystal structure, modifies the broad AuNP absorption giving rise to the unusual line shape observed. These results show new properties of opals infiltrated with active materials which can be exploited for nanophotonic applications.

Acknowledgment. We acknowledge support from the Italian Ministry of Instruction, University and Research through projects PRIN nos. 2004035502, 2004033197, 2006031511 and FIRB RBNE019NKS. We also thank Prof. L.C. Andreani for providing us the code for photonic band structure calculations.

References and Notes

- (1) Lopez, C. *Adv. Mater.* **2003**, *15*, 1679.
- (2) Moroz, A. *Mat. Res. Soc. Symp. Proc.* **2002**, *708*, K7.5.
- (3) Moroz, A. *Europhys. Lett.* **2000**, *50*, 466.
- (4) Kamaev, V.; Kozhevnikov, V.; Vardeny, Z. V.; Landon, P. B.; Zakhidov, A. A. *J. Appl. Phys.* **2004**, *95*, 2947.
- (5) Freymann, G. v.; John, S.; Schulz-Dobrick, M.; Vekris, E.; Tetreault, N.; Wong, S.; Kitaev, V.; Ozin, G. A. *Appl. Phys. Lett.* **2004**, *84*, 224.
- (6) Wang, D.; Salgueirino-Maceira, V.; Liz-Marzan, L. M.; Caruso, F. *Adv. Mater.* **2002**, *14*, 908.

- (7) Wang, D.; Li, J.; Chan, C. T.; Salgueirino-Maceira, V.; Liz-Marzan, L. M.; Romanov, S.; Caruso, F. *Small* **2005**, *1*, 122.
- (8) Morandi, V.; Marabelli, F.; Amendola, V.; Meneghetti, M.; Comoretto, D. *Adv. Func. Mater.* **2007**, *17*, 2770.
- (9) Rodriguez-Gonzales, B.; Salgueirino-Maceira, V.; Garcia-Santamaria, F.; Liz-Marzan, M. *Nano Lett.* **2002**, *2*, 471.
- (10) Wang, W.; Asher, S. A. *J. Am. Chem. Soc.* **2001**, *123*, 12528.
- (11) Tan, Y.; Qian, W.; Ding, S.; Wang, Y. *Chem. Mater.* **2006**, *18*, 3385.
- (12) Kulinowski, K. M.; Jiang, P.; Vaswani, H.; Colvin, V. L. *Adv. Mater.* **2000**, *12*, 833.
- (13) Tessier, P. M.; Velev, O. D.; Kalamur, A. T.; Lenhoff, A. M.; Rabolt, J. F.; Kaler, E. W. *Adv. Mater.* **2001**, *13*, 396.
- (14) Miclea, P. T.; Susha, A. S.; Liang, Z.; Caruso, F.; Torres, C. M. S.; Romanov, S. G. *Appl. Phys. Lett.* **2004**, *84*, 3960.
- (15) Romanov, S. G.; Susha, A. S.; Sotomayor-Torres, C. M.; Liang, Z.; Caruso, F. *J. Appl. Phys.* **2005**, *97*, 086103.
- (16) John, S. *Phys. Rev. Lett.* **1987**, *58*, 2486.
- (17) Vlasov, Y. A.; Kaliteevski, M. A.; Nikolaev, V. V. *Phys. Rev. B* **1999**, *60*, 1555.
- (18) Galisteo-Lopez, J. F.; Galli, M.; Andreani, L. C.; Mihi, A.; Pozas, R.; Ocana, M.; Miguez, H. *Appl. Phys. Lett.* **2007**, *90*, 101113.
- (19) Joannopoulos, J. D.; Meade, R. D.; Win, J. N. *Photonic Crystals: Molding the Flow of the Light*; Princeton University Press: Princeton, NJ, 1995.
- (20) Amendola, V.; Rizzi, G. A.; Polizzi, S.; Meneghetti, M. *J. Phys. Chem. B* **2005**, *109*, 23125.
- (21) Amendola, V.; Polizzi, S.; Meneghetti, M. *J. Phys. Chem. B* **2006**, *110*, 7232.
- (22) Amendola, V.; Polizzi, S.; Meneghetti, M. *Langmuir* **2007**, *23*, 6766.
- (23) Amendola, V.; Meneghetti, M. *J. Mater. Chem.* **2007**, *17*, 4705.
- (24) Pokrovsky, A. L.; Kamaev, V.; Li, C. Y.; Vardeny, Z. V.; Efros, A. L.; Kurdyukov, D. A.; Golubev, V. G. *Phys. Rev. B* **2005**, *71*, 165114.
- (25) Moroz, A. *Phys. Rev. Lett.* **1999**, *83*, 5274.
- (26) Transmittance spectra in Figure 2 are reported in arbitrary units to better compare spectra for thin AuNP doped opals with much thicker bare ones in particular for what concerns the spectral shift due to infiltration and the shape of spectra.
- (27) As we showed in a previous paper (see *Adv. Func. Mater.* **2007**, *17*, 2770) the random distribution of AuNP inside the highly doped opals interstices removes the symmetry of the system thus making the photonic band structure unaffected by light polarization, conversely from that observed in bare opals (see *Appl. Phys. Lett.* **2002**, *82*, 4068 (03) and references cited therein). For this reason, we report in this paper the dispersion of the spectra for TE polarization only. Data for TM polarization are identical within experimental error for all samples investigated.
- (28) Vos, W. L.; Sprik, R.; Blaaderen, A. v.; Imhof, A.; Lagendijk, A.; Wegdam, G. H. *Phys. Rev. B* **1996**, *53*, 16231.
- (29) The dielectric constant of interstices partially filled with AuNP is determined by inversion of the Lorentz–Lorenz–Lorenz, effective medium formula by using n_{eff} values determined from the Bragg–Snell fit as an input, being $n = 1.59$ for PS microspheres. This method was previously discussed in: *Adv. Func. Mater.* **2007**, *17*, 2770.
- (30) The PBG structure has been calculated with a code based on the plane wave expansion (see Pavarini, E.; et al. *Phys. Rev. B* **2005**, *72*, 045102). Input data of this code are the sphere diameter, the lattice type, the volume fraction (compact in our case), and the real dielectric constant of sphere and interstices. The calculation gives a rough estimate of the position of the photonic band of the opal since it neglects the dispersion of the refractive index and the imaginary part of the dielectric function [see Joannopoulos, J. D.; Meade, R. D.; Win, J. N. *Photonic Crystals: Molding the Flow of the Light*; Princeton University Press: Princeton, NJ, 1995]. However, a careful analysis of the reflectance spectra shows that in the spectral range of surface plasmon resonance, no spectral features are observed except the interference fringes having an intensity less than 1% and noise level less 0.3% with respect to the photonic stop band. This sets the upper sensitivity limit for plasmon band intensity and means that the intensity of the plasmon band is at least more than 30 times lower than that of the stop band. This implies a relatively low absorption of AuNP. In fact, the only minor suggestion for the presence of an absorption is provided by the reduction of reflectance background for photon energies immediately below the stop band. This fact makes us confident that our band structure calculation is, as a first approximation, reasonable and the effect of absorption can be treated as a perturbation and then interpreted in a qualitative way.
- (31) Huang, J.; Eradat, N.; Raikh, M. E.; Vardeny, Z. V.; Zakhidov, A. A.; Baughman, R. H. *Phys. Rev. Lett.* **2001**, *86*, 4815.
- (32) Vlasov, Y. A.; Astratov, V. N.; Baryshev, A. V.; Kaplyanskii, A. A.; Karimov, O. Z.; Limonov, M. F. *Phys. Rev. E* **2000**, *61*, 5784.
- (33) Romanov, S. G.; Maka, T.; Torres, C. M. S.; Muller, M.; Zentel, R. *J. Appl. Phys.* **2002**, *91*, 9426.
- (34) Vlasov, Y. A.; Deutsch, M.; Norris, D. J. *Appl. Phys. Lett.* **2000**, *76*, 1627.
- (35) Popov, O.; Lirtsman, V.; Kopnov, F.; Davidov, D.; Saraidarov, T.; Reisfeld, R. *Synth. Met.* **2003**, *139*, 643.
- (36) Huang, J. D.; Raikh, M.; Eradat, N.; Vardeny, Z. V.; Zakhidov, A. A.; Baughman, R. H. *Synth. Met.* **2001**, *116*, 505.
- (37) Galisteo-Lopez, J. F.; Galli, M.; Patrini, M.; Balestreri, A.; Andreani, L. C.; Lopez, C. *Phys. Rev. B* **2006**, *73*, 125103.
- (38) Galisteo-Lopez, J. F.; Palacios-Lidon, E.; Castillo-Martinez, E.; Lopez, C. *Phys. Rev. B* **2003**, *68*, 115109.
- (39) Eradat, N.; Sivachenko, A. Y.; Raikh, M. E.; Vardeny, Z. V.; Zakhidov, A. A.; Baughman, R. H. *Appl. Phys. Lett.* **2002**, *80*, 3491.
- (40) Sumioka, K.; Nagahama, H.; Tsutsui, T. *Appl. Phys. Lett.* **2001**, *78*, 1328.
- (41) Sivachenko, A. Y.; Raikh, M. E.; Vardeny, Z. V. *Phys. Rev. A* **2001**, *64*, 013809.
- (42) Huang, K. C.; Bienstman, P.; Joannopoulos, J. D.; Nelson, K. A.; Fan, S. *Phys. Rev. Lett.* **2003**, *90*, 196402.
- (43) Huang, K. C.; Bienstman, P.; Joannopoulos, J. D.; Nelson, K. A.; Fan, S. *Phys. Rev. B* **2003**, *68*, 075209.
- (44) Huang, K. C.; Lidorikis, E. X.; Jiang, J. D. J.; Nelson, K. A. *Phys. Rev. B* **2004**, *69*, 195111.
- (45) Centini, M.; Sibilia, C.; Scalora, M.; D'Aguanno, G.; Bertolotti, M.; Bloemer, M. J.; Bowden, C. M.; Nefedov, I. *Phys. Rev. E* **1999**, *60*, 4891.
- (46) Scalora, M.; Dowling, J. P.; Bowden, C. M.; Bloemer, M. J. *Phys. Rev. Lett.* **1994**, *73*, 1368.
- (47) Bulu, I.; Caglayan, H.; Ozbay, E. *Phys. Rev. B* **2003**, *67*, 205103.
- (48) Vlasov, Y. A.; Luterova, K.; Pelant, I.; Honerlage, B.; Astratov, V. N. *Appl. Phys. Lett.* **1997**, *71*, 1616.
- (49) Dowling, J. P.; Scalora, M.; Bloemer, M. J.; Bowden, C. M. *J. Appl. Phys.* **1994**, *75*, 1896.